Ocean Engineering 340 (2025) 122226

Contents lists available at ScienceDirect

Ocean Engineering

journal homepage: www.elsevier.com/locate/oceaneng

Research paper

Effect of plate-stiffener combination modelling uncertainty on ship's hull girder ultimate strength reliability in vertical bending

Shen Li [a,*], Jeom Kee Paik [b,c,d,e], C. Guedes Soares [f], Dimitris G. Georgiadis [g], Do Kyun Kim [h,**]

[a] Department of Naval Architecture, Ocean and Marine Engineering, University of Strathclyde, UK
[b] Department of Mechanical Engineering, University College London, London, UK
[c] Faculty of Maritime and Transportation, Ningbo University, Ningbo, China
[d] Yantai Research Institute of Harbin Engineering University, Yantai, China
[e] Hangzhou City University Binjiang Innovation Center, Hangzhou, China
[f] Centre for Marine Technology and Ocean Engineering (CENTEC), Instituto Superior Técnico, Universidade de Lisboa, Lisboa, Portugal
[g] Engineering Risk Analysis Group, Technical University of Munich, Germany
[h] Department of Naval Architecture and Ocean Engineering, Seoul National University, South Korea

ARTICLE INFO

Keywords:
Ultimate hull girder strength
Plate-stiffener combination (PSC) model
Ultimate strength-based reliability
Modelling uncertainties
Vertical bending

ABSTRACT

Vertical bending moment, resulting from uneven weight distribution, buoyancy, and dynamic wave forces, is a primary load component influencing ship hull structures. In extreme conditions, excessive bending can exceed a hull girder's ultimate strength, potentially causing catastrophic failure, commonly referred to as "breaking of its back." Assessing the ultimate capacity of ship hull girders is therefore critical for modern safety design practices. Hull structures, typically composed of stiffened panels, are often simplified into assemblies of "plate-stiffener combination" (PSC) models for efficient performance evaluation. These models approximate the behaviour of continuous stiffened plated structures under specific loads, making them a widely used approach for hull girder capacity analysis. While PSC models are effective for evaluating vertical bending moments, uncertainties arise due to variations in configurations, stress-strain relationships, or load-shortening curves. These factors influence local failures of plating, stiffener webs, and stiffener flanges, as well as their interactions. This paper quantifies the modelling uncertainties in PSC-based analyses of ultimate strength and reliability of ship hull structures. Based on multiple empirical formulae and 63 representative structural configurations, the derived uncertainty factor for PSC elements follows a log-normal distribution with a logarithmic mean of 0.087 and standard deviation of 0.1. A new formulation of limit state function is introduced to accommodate these uncertainties. The proposed approach is demonstrated through illustrative examples involving an ultra-large container ship and the Dow's frigate. It was found that the inclusion of PSC elements' modelling uncertainty represents a considerable reduction in reliability index ranging from 2.5 % to 15 %. The proposed framework provides a practical method for embedding strength modelling uncertainty into ultimate strength-based reliability assessments.

1. Background

Ships and ship-form offshore assets are vital to modern society, serving as critical infrastructures in maritime transport and ocean energy sectors (Paik, 2022). These assets function as multi-disciplinary systems, with the hull structures acting as a sub-system that provides a physical means to integrate other sub-systems while providing essential protection (Hughes and Paik, 2010). While ship hull structures face various hazards existing in the marine environment (Paik, 2020), significant advancements in research on these structures have enabled comprehensive limit state assessments (Bai and Paik, 2024; Paik, 2020). This study specifically addresses the Ultimate Limit State (ULS), where structural adequacy is verified against extreme loading conditions (Bai and Paik, 2024; Paik, 2018; Kim et al., 2013a,b; Paik et al., 2012). Failure under such loading, often referred to as "breaking of the back", has led to several well-known maritime accidents, including the *Energy Concentration* collapse in 1980, the *Erika* collapse in 1999, the *Prestige* collapse in 2002, the *MSC Napoli* collapse in 2007, and the *MOL Comfort*

* Corresponding author.
** Corresponding author.
E-mail addresses: shen.li@strath.ac.uk (S. Li), do.kim@snu.ac.kr (D.K. Kim).

https://doi.org/10.1016/j.oceaneng.2025.122226
Received 16 December 2024; Received in revised form 8 July 2025; Accepted 16 July 2025
Available online 23 July 2025

collapse in 2013. More recently, in 2021, the *MV Arvin* broke in two and sank in heavy seas off the coast of Bartin, Turkey. Although the likelihood of hull girder collapse is relatively low compared to other failure modes, its severe consequences make it a key consideration in the risk-based structural design of ships and offshore structures.

The main bodies of ship hull structures are often modelled as assemblies of simplified engineering elements with idealised behaviours under specific load applications, and collectively, the assembly mimics the behaviour of the actual structures. Common examples of such structural idealisations for modelling continuous stiffened plate structures include the Plate-Stiffener Combination (PSC) model (also called the beam-column model), the Plate-Stiffener Separation (PSS) model, the orthotropic plate model, and the Supersize Finite (plate) Element (segment) model, and the refined Finite (plate) Element model. These models are discussed in Paik (2018). For predicting the progressive collapse of hull girders, average stress-average strain relationships or load-shortening curves of these simplified models are formulated, with hull girder loads applied incrementally. Smith (1977) initially proposed this approach for vertical bending based on PSC elements, which is now incorporated in contemporary marine structural design code (IACS, 2019). To enhance analytical accuracy, hull structures are often idealised using plate-stiffener separation (PSS) models, treating them as assemblies of local plating elements and reinforcements (e.g., stiffeners). This approach, initially known as the Idealised Structural Unit Method (ISUM), was generalised into the Intelligent Supersize Finite Element Method (ISFEM) by Paik (2018).

To account for uncertainties in strength assessments, probabilistic methods have been introduced. Nevertheless, a remaining challenge is the presence of implicit and unquantified uncertainties, or safety factors, which contribute to an indeterminate level of conservatism in these assessments. This approach is adequate for safety-focused design, where the principal objective is to prevent failure rather than precise prediction of failure. Nevertheless, if these assessments prioritise optimising resilience and resource allocation over simply demonstrating safety, more informative and precise reliability estimates will become crucial (Francesco et al., 2022). This shift is arguably urgent given recent budget constraints of the sector, as well as the growing emphasis on structural optimisation to meet emission reduction targets. This paper focuses on examining the modelling uncertainties inherent in PSC models (Guedes Soares, 1988) aligned with the structural modelling techniques outlined in IACS (2019). Traditionally, uncertainties in hull girder structural capacity are amalgamated into a single model uncertainty factor, which is used as a multiplier in global capacity estimates for structural reliability analysis (e.g., Parunov and Guedes Soares, 2008; Gaspar et al., 2016). However, quantifying this uncertainty remains challenging due to the limited availability of global capacity data. To improve the treatment of strength model uncertainty in structural reliability analysis, this paper introduces a methodology to address modelling uncertainties in formulating load-shortening curves using more accessible data (Paik et al., 2020; Liu et al., 2021, 2022). The developed method parameterizes the load-shortening curves of PSC elements to characterize their stress-strain relations under the incremental application of corresponding vertical bending. Modelling uncertainties (χ_e) are introduced as multipliers associated with behavioural characteristics of PSC elements, such as the ultimate compressive strength. By modifying the key behavioural characteristics, the uncertainty in the load-shortening curve (LSC) is accounted for before it is used in the incremental hull girder analysis. The original uncertainty factor remains to address uncertainties related to element discretisation and other modelling assumptions, such as the assumption that the cross-section remains plane.

The rest of this paper is structured as follows. A selective overview of the relevant advancements in progressive collapse analysis and reliability-based design is presented in Section 2. Section 3 outlines the proposed methodology for incorporating PSC modelling uncertainty into an ultimate strength-based reliability assessment. Section 4 discusses the case study results on an ultra-large container ship and the Dow's frigate. Finally, concluding remarks are provided in Section 5.

2. STATE-OF-THE-ART review

A focused overview is provided in this section for the various methods that have been developed for the progressive collapse analysis of ship hull structures, and probabilistic methods and reliability-based design for these structures.

2.1. Progressive collapse analysis of ship hull structures

A substantial body of methodologies has been developed to simulate the progressive collapse behaviour and calculate the ultimate strength of ship hull structures under vertical bending, with the first analytical approach developed by Smith (1977). Methodologies based on similar principles were also developed by Adamchak (1982) and Gordo and Guedes Soares (1996). Over time, the original method has been extended to address various structural configurations and loading conditions, each extension adding unique capabilities for specific applications.

Smith and Dow (1986) extended the method to accommodate combined vertical and horizontal bending by introducing a coupled flexural equation that accounts for interactions between these bending modes. This extended formulation also provides a foundation for analysing damaged ship hull structures with asymmetric cross-sections, as later developed by Dow (1997) and Fujikubo et al. (2012). Benson et al. (2013) developed a compartment-level progressive collapse analysis methodology, effectively removing the inter-frame collapse assumption in the original approach. Li et al. (2019, 2020) further advanced the original method's applicability to predict the collapse behaviour of ship hull structures subjected to extreme cyclic bending load. Tatsumi et al. (2020) adapted the original method to incorporate combined hogging moments and local bottom loads, an extension particularly relevant for container ships. Li et al. (2021a) extended the original method by adopting Timoshenko beam formulation and considering shear lag, which effectively addresses the assumption that cross-sectional plane remains plane when subjected to vertical bending. Collectively, these extensions have greatly broadened the original method's scope, enhancing its ability to assess the progressive collapse behaviour and ultimate strength of ship hull structures under complex loading scenarios.

The aforementioned methodologies are predominantly based on PSC modelling. Extensive research also exists on progressive collapse analysis of hull structures idealised as PSS elements, initially within the framework of ISUM and later generalised as the ISFEM. Unlike the traditional finite element method (FEM), ISFEM pre-defines the nonlinear behaviour of its elements (Paik, 2018). This approach is advantageous for simulating the nonlinear, progressive collapse behaviour of complex structures, such as ship hulls, as it offers computational efficiency while preserving the foundational framework of FEM. In terms of ISFEM's application, Kim et al. (2013a,b) developed the residual strength-grounding damage index diagram for tankers subjected to grounding damage using the ISFEM. Li and Kim (2022) compared this ISFEM-based diagram with those developed using PSC element-based incremental hull girder analysis. Magoga and Flockhart (2014) employed ISFEM to assess the ultimate hull-girder strength under vertical and horizontal bending of the midship section of an aluminium high-speed patrol vessel. Their analysis explored the impact of weld-induced imperfections such as geometric distortion and residual stresses on ultimate strength. Similarly, Youssef et al. (2016, 2017) and Faisal et al. (2017) utilised ISFEM to simulate the progressive collapse behaviour of hull girders subjected to various collision damages. Additionally, Zhang et al. (2016) applied ISFEM to explore the shakedown limit state of hull girders, suggesting that ship hulls under cyclic vertical bending may experience the shakedown phenomenon, despite the

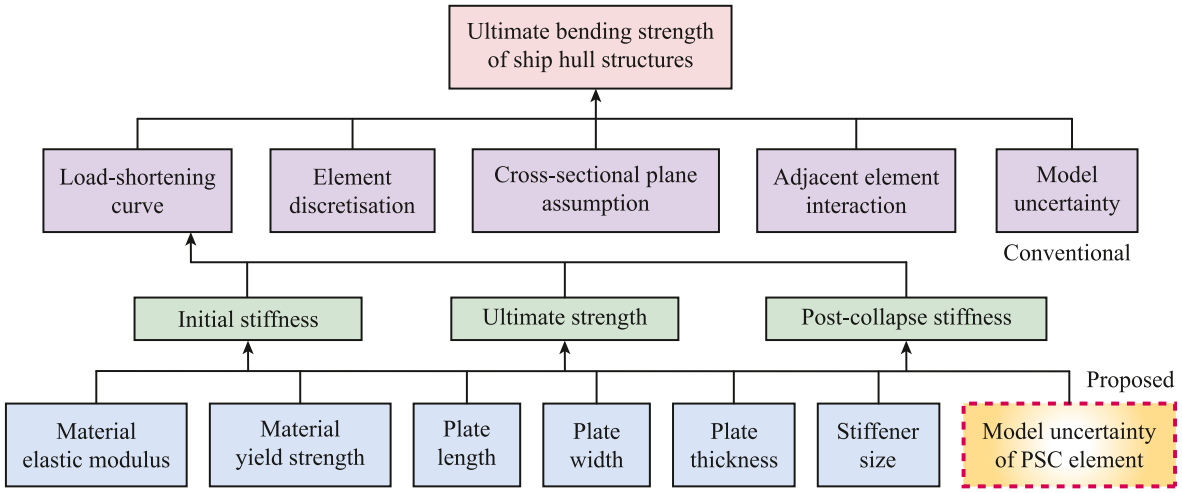

Fig. 1. Modelling of ultimate bending strength of ship hull structures in terms of input-output relationships.

applied vertical bending moments remain below the ultimate hull girder strength determined under static loads.

2.2. Reliability-based design of ship hull structures

While probabilistic methods and reliability-based design have been extensively studied and applied in civil, aeronautics, and aerospace engineering structures, their applications to ships and ship-shaped offshore structures likely began with the pioneering efforts of Mansour (1972) and Faulkner and Sadden (1979) primarily employing Level-2 second moment approach. These works have been motivated by the shortcomings in conventional safety factor approaches (Level-1 approach), which may impede optimal weight and cost efficiency. In the years that followed, several complementary studies were conducted to quantify the uncertainties associated with still-water bending loads, wave-induced bending loads, and their combination (Guedes Soares and Moan, 1982; Wang and Moan, 1996; Baarholm and Moan, 2000). Additionally, systematic surveys were undertaken to address strength modelling uncertainties related to material and geometric variabilities (Hughes, 1994; Guedes Soares, 1988; Hess et al., 2002). These early efforts have significantly shaped the present-day research on the reliability-based design of ships and offshore structures (Paik and Frieze, 2001).

Recent years have seen continued advancements. Parunov and Guedes Soares (2008) employed reliability analysis to assess changes in safety levels resulting from the redesign of an existing Aframax tanker to meet the Common Structural Rules (CSR) requirements. Shu and Moan (2011) evaluated the ultimate limit state reliability of a bulk carrier, focusing on two typical load cases: pure longitudinal bending in hogging and combined longitudinal bending in hogging with local lateral pressure loads. Gaspar et al. (2016) examined the impact of nonlinear vertical wave-induced bending moments on reliability evaluation. Parunov et al. (2020) investigated the structural reliability of damaged ship hull structures subjected to collision, comparing how different damage modelling approaches affect failure probability. Time-dependent degradation has also been a key focus. Liu et al. (2019) developed a risk analysis framework that incorporates hull girder reliability, life-cycle cost, and the availability of aging ship structures under fatigue deterioration. Gong and Frangopol (2020) proposed a time-variant reliability formulation for ship hull girders subjected to corrosion, incorporating the spatial variability of corrosion growth and the geometric and material properties of structural elements. A range of copula models were utilised to model the joint probability distribution of these spatially dependent variables.

2.3. Remarks on the state-of-the-art and challenges

Difficulties that hindered the early application of probabilistic methods and reliability-based design, as discussed by Goodman (1979) and Moan (1979), include: (1) the lack of general consensus on how to integrate the various elements of the safety concept into a practical methodology that yields stable and consistent results; and (2) although the primary advantage of probabilistic methods lies in their ability to systematically account for uncertainties and variabilities, a major challenge has been the identification and quantification of inherent uncertainty, which arises from the natural variability of basic variables such as geometric parameters and material properties; model uncertainty, which stems from the inadequacy or imperfection of the engineering model; and statistical uncertainty, which results from limited data availability, such as a small sample size. Research over the past few decades has significantly advanced the integration of computational models and improved the information availability, enabling engineers in ship and offshore structures to conduct such analyses more effectively. However, uncertainty quantification remains an open-ended challenge, warranting continued research efforts. The introduction of new materials, novel structural solutions, manufacturing technologies, and operational requirements (such as changing environmental conditions) suggests that previously developed databases on strength and load modelling may no longer be adequately representative for emerging applications.

Regarding the uncertainty in structural strength modelling, which is the focus of the present work, the reviewed literature typically addresses ultimate strength uncertainty using a single model uncertainty factor. As shown in Fig. 1, this conventional approach (i.e., the use of χ_u, introduced in Section 3) is intended to implicitly account for all uncertainties in the modelling aspects of progressive collapse analysis and ultimate bending strength computation, such as load-shortening curve formulation, element discretisation, and assumptions inherent in the incremental approach. However, this factor is often based primarily on engineering judgement rather than systematic evaluation. Recently, Xu et al. (2015) proposed a model correction approach that uses an iterative procedure to correct the strength model based on a more sophisticated prediction (assumed to represent the realistic value). In Xu's method, nonlinear finite element analysis predictions were utilised for model correction. Georgiadis et al. (2023) quantified strength model uncertainty using Bayesian inference. The estimation of parameters characterising the probabilistic model of the uncertainty factor were enhanced by finite element simulation results. However, these efforts remain focused on the model uncertainty factor at the hull girder response hierarchy level. Explicit consideration of model uncertainty for the

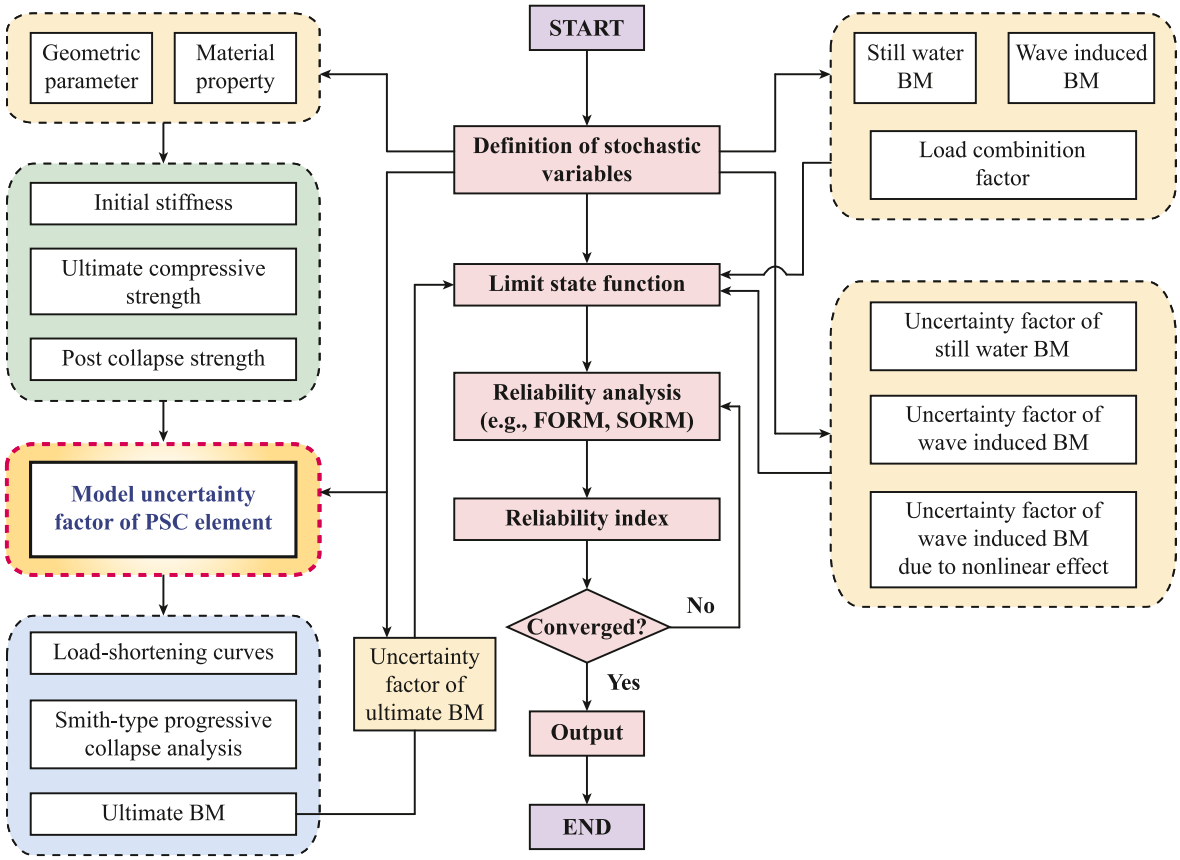

Fig. 2. Proposed methodology for calculating ultimate strength reliability under vertical bending.

responses of local structural components, such as PSC elements, within the framework of ultimate strength reliability for hull girders, is notably absent from the literature (Li et al., 2022). This paper addresses this gap by introducing a modelling uncertainty factor for PSC elements (χ_e, introduced in Section 3).

3. Methodology

3.1. Principles

The overall methodology adopted in this work for calculating the ultimate hull girder strength reliability under vertical bending is depicted in Fig. 2. It broadly follows the standard framework for structural reliability analysis of ship hull girders. The process begins with the identification of stochastic variables, including structural geometry and material properties (used in calculating the ultimate load-carrying capacity), and environmental loads (still water bending moment and wave-induced bending moment in this study). Modelling uncertainties associated with both structural strength and environmental loads are also explicitly included. These basic variables are then used to define a limit state function that characterises failure based on a prescribed failure mode. In this case, the limit state function is implicit. While environmental loads are defined explicitly, the ultimate strength is calculated using an analytical method. Specifically, the Smith-type progressive collapse analysis is adopted, which incrementally estimates the ultimate bending strength of the hull girder. With the limit state function established, reliability analysis is conducted to quantify the failure probability. Among various available methods, the First-Order Reliability Method (FORM) is employed, using the concept of reliability index. A concise introduction to aforementioned techniques is presented in Sections 3.3-3.6.

The novelty of this work lies in the inclusion of uncertainty in the formulation of load-shortening curves, which is a critical component in the Smith-type progressive collapse analysis used to determine the ultimate bending strength. Building upon numerous research, the ultimate limit state function for ship's hull girder in vertical bending can be given as follows (Guedes Soares et al., 1996):

$$g(\boldsymbol{X}) = \chi_u M_u(\boldsymbol{X}) - (\chi_{sw} M_{sw} + \Psi \chi_w \chi_{nl} M_w) \tag{1}$$

where M_u is the ultimate bending strength of hull girder and is a function of geometric parameters and material properties $\boldsymbol{X} = \{a, b, t, h_w, t_w, b_f, t_f, \sigma_Y, E\}$. M_{sw} is the still water bending moment, M_w is the wave-induced bending moment, χ_u, χ_{sw}, χ_w and χ_{nl} are the uncertainty factors for M_u, M_{sw}, M_w and nonlinear effect of M_w. Ψ is the load combination factor to consider the fact that the maxima of M_{sw} and M_w do not occur simultaneously. M_u is calculated by the incremental procedure outlined in IACS based on PSC elements characterized by load-shortening curves (LSCs, $f_{\sigma-\varepsilon}$):

$$g(\boldsymbol{X}) = \chi_u M_u[f_{\sigma-\varepsilon}(\boldsymbol{X})] - (\chi_{sw} M_{sw} + \Psi \chi_w \chi_{nl} M_w) \tag{2}$$

More detailed description of the procedure for calculating ultimate bending strength (M_u) is provided in Section 3.3. As per Li et al. (2021b), LSC modelling can simplify to determine the initial stiffness $E_{T_o}(\boldsymbol{X})$, the ultimate compressive strength $\sigma_u(\boldsymbol{X})$, and the post-collapse strength at 1.5 times of the ultimate strain $\sigma_{1.5\varepsilon_u}(\boldsymbol{X})$ and at 2.0 times of the ultimate strain $\sigma_{2.0\varepsilon_u}(\boldsymbol{X})$:

$$\sigma = f_{\sigma-\varepsilon}[E_{T_o}(\boldsymbol{X}), \sigma_u(\boldsymbol{X}), \sigma_{1.5\varepsilon_u}(\boldsymbol{X}), \sigma_{2.0\varepsilon_u}(\boldsymbol{X})] \tag{3}$$

Considering only the uncertainty of ultimate compressive strength $\sigma_u(\boldsymbol{X})$:

$$\sigma = f_{\sigma-\varepsilon}[E_{T_o}(\boldsymbol{X}), \chi_e \sigma_u(\boldsymbol{X}), \sigma_{1.5\varepsilon_u}(\boldsymbol{X}), \sigma_{2.0\varepsilon_u}(\boldsymbol{X})] \tag{4}$$

where χ_e is the model uncertainty factor related to the ultimate

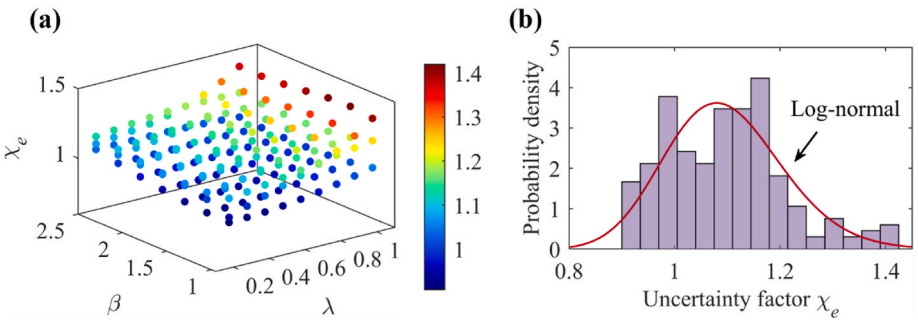

Fig. 3. (a) Database of uncertainty factor χ_e; (b) Fitted probability distribution.

compressive strength of PSC elements. Inserting Equation (4) into Equation (2), the updated limit state function read as follows:

$$g(\boldsymbol{X}) = \chi_u M_u\{f_{\sigma-\varepsilon}[E_{T_0}(\boldsymbol{X}), \chi_e\sigma_u(\boldsymbol{X}), \sigma_{1.5\varepsilon_u}(\boldsymbol{X}), \sigma_{2.0\varepsilon_u}(\boldsymbol{X})]\} - (\chi_{sw}M_{sw} + \Psi\chi_w\chi_{nl}M_w) \tag{5}$$

The quantification of the uncertainty factor χ_e is introduced in Section 3.2. It is important to reiterate that the model uncertainty factor χ_e is embedded in the calculation of M_u, rather than being applied as an additional multiplier to M_u. The original uncertainty factor for ultimate bending capacity (χ_u) remains in the updated limit stated function, accounting for model uncertainty arising from factors such as the limitations of incremental method based on PSC models. In reality, a stiffened plate structure reaches the ultimate strength involving the interaction between a number of elastoplastic buckling failure modes. PSC models are inherently inadequate for accurately representing this complex interaction. The use of PSS model can address this issue.

3.2. Uncertainty quantification for ultimate compressive strength of PSC elements

For the derivation of uncertainty factor χ_e which addresses the model uncertainty of ultimate compressive strength prediction, four widely recognised empirical formulae are selected: Paik and Thayamballi (1997), Zhang and Khan (2009), Xu et al. (2018), and Kim et al. (2017). These models are considered representative of established approaches in the literature and were chosen based on the authors' judgement of their prevalence and diversity in analytical foundations, and thus approximating the uncertainty associated with behavioural characterization of PSC elements. These formulae are all expressed in terms of two non-dimensionless parameters: plate slenderness ratio (β) and column slenderness ratio (λ), given as follows:

$$\beta = \frac{b}{t_p}\sqrt{\frac{\sigma_Y}{E}} \tag{6a}$$

$$\lambda = \frac{a}{\pi r}\sqrt{\frac{\sigma_Y}{E}} \tag{6b}$$

where a is the panel length, b is the plate width, t_p is the plate thickness, σ_Y is the material yield strength, E is the Young's modulus and $r = \sqrt{I/A}$ with I being the area moment of inertia and A being the cross-sectional area. The dataset comprises 7 slenderness ratio ($\beta = 1.0, 1.25, 1.5, 1.75, 2.0, 2.25, 2.5$) and 9 column slenderness ratio ($\lambda = 0.2, 0.3, 0.4, 0.5, 0.6, 0.7, 0.8, 0.9, 1.0$), thus in total 63 combinations of plate and column slenderness ratios (a full summary is provided in the Appendix). These ranges are consistent with the statistical distribution of structural parameters in ship hull configurations reported by Zhang and Khan (2009) and are considered representative of realistic PSC elements in marine structures. For each configuration, ultimate strength is computed using all four formulae. These structural configurations are regarded as representative of ship hull structures. The prediction derived from the Paik-Thayamballi formula (σ_{xu}^{P-T}) is selected as the baseline. Predictions from the other three formulae (σ_{xu}^{others}) are compared against this baseline to determine the prediction bias, which is considered as the uncertainty factor χ_e in this illustrative example.

$$\chi_e = \frac{\sigma_{xu}^{others}}{\sigma_{xu}^{P-T}} \tag{7}$$

The Paik and Thayamballi formula was selected as the baseline primarily because it was the earliest among the four and is based on experimental data, whereas the others were derived from finite element analyses. In fact, any of the selected formula or a new finite element analysis or additional experimental data could serve as the baseline. However, it was opted not to perform new finite element simulations, and this decision was based on the consideration that some of the selected formulae were themselves derived from detailed FE simulations and already reflect those methodologies. Therefore, conducting further simulations was deemed to add limited value within the scope of this work. Moreover, the aim of this study is not to claim that any one formula is definitively correct and the derived uncertainty factor is universally representative, but to propose a methodology that explicitly accounts for the uncertainty introduced by differing predictive models, which is a factor that has often been handled empirically or embedded implicitly within a single safety factor, typically without a clear or traceable basis. With three comparisons per configuration, a total of 189 data points is collected (Fig. 3a). Since no prior knowledge is available regarding the probability distribution of model uncertainty factor χ_e, the data is fitted to five different types of probability distributions: normal, log-normal, Weibull, extreme value and exponential. The Bayesian Information Criterion (BIC) is computed for each fitted distribution to guide model selection, with lower BIC values indicating better fit. The BIC balances two competing goals: achieving a good fit to the data and avoiding overfitting by penalising model complexity. The log-normal distribution, with a logarithmic mean of 0.087 and a standard

Table 1
Probability distribution fitting results.

Probability distribution	Bayesian information criterion
Log-normal	−292.27
Normal	−283.75
Weibull	−248.50
Extreme value	−224.17
Exponential	414.92

Table 2
Effect of sampling number on the statistics of uncertainty factor χ_e

Number of sample configurations	Number of data points	Mean	Coefficient of Variation
63	189	1.097	0.103
144	432	1.096	0.103
527	1581	1.095	0.100

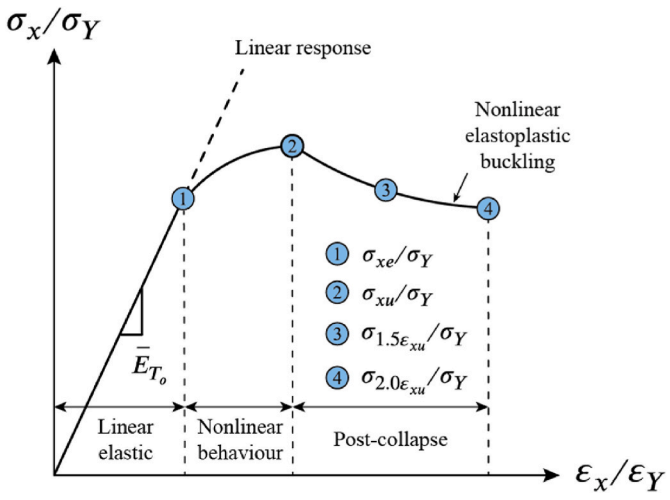

Fig. 4. Schematic illustration of load-shortening curve modelling of PSC elements.

deviation of 0.1 (Fig. 3b), is found to have the smallest BIC value and therefore is identified as the best-fit distribution. A summary of the Bayesian Information Criterion values for all candidate distributions is provided in Table 1. To assess the robustness of this approach, additional analyses were conducted using finer sampling grids (144 and 527 configurations, and thus 432 and 1581 data points, respectively). As summarised in Table 2, the resulting changes in the statistical parameters of χ_e were negligible, suggesting that the adopted 63-case grid is sufficient for the purposes of this illustrative study.

It is acknowledged that the selection of empirical formula in this study is based on engineering judgement, and further investigation is required to improve the representativeness of the resulting uncertainty factor. As discussed in Section 4.3, a collaborative benchmark study would be a valuable step toward more robust and comprehensive uncertainty quantification. The main aim of the proposed framework is to offer a practical means of incorporating the modelling uncertainty associated with the PSC elements into hull girder reliability analysis.

3.3. Incremental hull girder analysis

The hull girder's ultimate strength under vertical bending is assessed using Smith-type progressive collapse analysis, following the IACS (2019) approach. The cross-section is idealised into PSC elements, each assigned a load-shortening curve (see Section 3.4), and the applied vertical moment is incremented iteratively. At each increment, the strain at each element is computed based on curvature, and the tangent stiffness is updated using the corresponding stress-strain response. The neutral axis is recalculated to reflect changes in stiffness distribution, and the section's moment-curvature relationship is progressively constructed until failure.

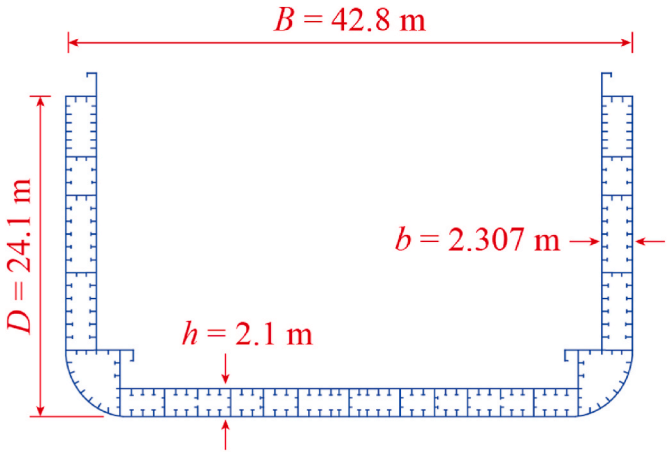

Fig. 5. Schematics of the mid-ship cross-section of container ship (detailed structural scantling information available in Mohammed et al. (2016)).

3.4. Load-shortening curve modelling

The method proposed by Li et al. (2021b) is utilised for modelling load-shortening curves (LSCs). This approach is based on an idealisation of predictions from numerical simulation and approximates the compressive LSC using idealised response characteristics: elastic stiffness of the initial response (E_{T_o}), ultimate collapse strength in compression (σ_{xu}), ultimate collapse strain (ε_{xu}), and the post-ultimate collapse unloading behaviour. Each characteristics can be tailored to specific conditions, e.g., uni-axial compression, bi-axial compression and combined compression and shear etc. Under uni-axial compression induced by vertical bending, the initial elastic stiffness is typically assumed to equal the material's elastic modulus, while the ultimate compressive strength can be determined using empirical formulas or advanced numerical simulations, such as NLFEM. In this study, the CSR method is employed as the base case. The ultimate strain is taken as the material yield strain for simplicity, which is also consistent with the CSR method (IACS, 2019). With respect to the post-collapse response, a bilinear response is considered and is determined by two variables (Post collapse strength $\sigma_{1.5\varepsilon_u}$ and $\sigma_{2.0\varepsilon_u}$ at 1.5 ε_u and 2.0 ε_u). A representation of the LSC model is shown in Fig. 4.

3.5. Vertical bending loads

The vertical bending moment acting on a ship hull girder consists of two primary components: still water bending moment (SWBM) and wave-induced vertical bending moment (VWBM). The SWBM results from the uneven distribution of the vessel's own weight and onboard cargo and is typically modelled as a normally distributed variable. Guedes Soares and Moan (1988) provided statistical evidence supporting this assumption based on a range of ship types. Hørte et al. (2007) further proposed a stochastic model for sagging SWBM with a mean and standard deviation of 70 % and 20 %, respectively, of the maximum SWBM defined in the loading manual. This approach was later extended to hogging conditions by Teixeira et al. (2013).

The VWBM is modelled using a long-term Weibull distribution calibrated to wave loading statistics, with extreme values represented by a Gumbel distribution to account for lifetime maxima. This approach is consistent with established methodologies reported by Xu et al. (2015), Parunov and Guedes Soares (2008), and Parunov et al. (2022).

3.6. First-order reliability method (FORM)

A first-order reliability method (FORM) is employed in this paper to approximate the probability of failure, i.e., $P_f = P[g(\boldsymbol{X}) < 0]$. The method is based on the concept of a reliability index, which provides a measure of safety in standard normal space (Rackwitz and Fiessler, 1978). The procedure begins by initialising a checking point based on the mean values of the stochastic variables. The limit state function and its partial derivatives with respect to each variable are then evaluated. As the limit state function is implicit in the present work, a central difference approximation is used to estimate the gradients. All non-normal variables are transformed into equivalent normal distributions at the current checking point. The reliability index is iteratively updated until convergence is achieved.

Table 3
Stochastic modelling of geometric parameters, material properties and uncertainty factors.

Variables	Symbol	Unit	Mean	COV	Distribution
Length of local plating	a	mm	Nominal	0.028	Normal
Width of local plating	b	mm	design	0.028	Normal
Thickness of local plating	t_p	mm	value	0.035	Log-normal
Web height of stiffener	h_w	mm		0.019	Normal
Web thickness of stiffener	t_w	mm		0.083	Gumbel
Flange width of stiffener	b_f	mm		0.016	Log-normal
Flange thickness of stiffener	t_f	mm		0.092	Gumbel
Yield strength	σ_Y	MPa		0.085	Log-normal
Elastic modulus	E	MPa		0.076	Normal
Model uncertainty factor for PSC elements	χ_e	–	0.087	0.10	Log-normal
Model uncertainty factor for M_u	χ_u	–	1.0	0.10	Normal
Model Uncertainty factor for M_{sw}	χ_{sw}	–	1.0	0.05	Normal
Model uncertainty factor for M_w	χ_w	–	1.0	0.10	Normal
Model uncertainty factor for M_w due to nonlinear effect	χ_{nl}	–	0.87	0.15	Normal
Load combination factor	Ψ	–	0.837	0.05	Normal

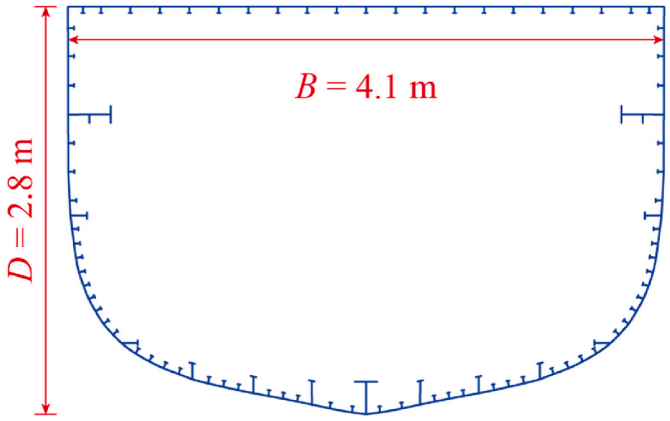

Fig. 6. Schematics of the mid-ship cross-section of Dow's frigate detailed structural scantling information available in Hughes and Paik (2010).

4. Illustrative example

4.1. Target ship hull structures

To illustrate the impact of PSC modelling on the structural reliability of hull girders under vertical bending, two case studies are analysed: an ultra-large container ship and the Dow's frigate model. The two hull girder models selected in this study represent two distinct categories of ship design: commercial and naval. Specifically, the ultra-large container ship is a typical example of a merchant vessel, characterised by a stockier hull form. In contrast, the Dow's frigate represents a naval vessel design, generally characterised by a slenderer design. These two examples were selected to provide contrasting, yet representative configurations commonly encountered in practice. This allows the proposed methodology to be demonstrated across a broader spectrum of hull structural characteristics. Detailed structural scantling information for the Dow's frigate is available in Hughes and Paik (2010), while that for the container ship is provided in Mohammed et al. (2016). Interested readers are directed to the cited sources where the complete structural data can be found.

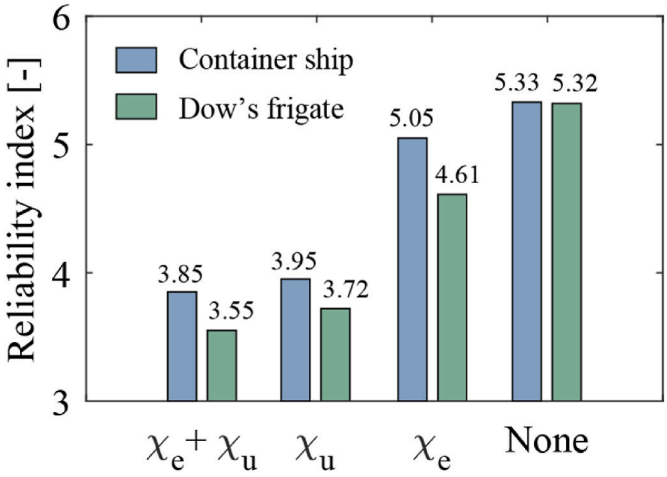

Fig. 7. Comparison of reliability index.

The container ship, depicted in Fig. 5, is analysed using a still water hogging bending moment with a mean value of 3.98 GNm and a coefficient of variation of 0.29, assuming a normal distribution. The maximum design wave-induced bending moment is 13.66 GNm, while extreme wave-induced bending moments over a one-year period are determined following the methodology described in Section 3.4. A summary of the stochastic variables is provided in Table 3. The Dow's frigate model (Dow, 1991), shown in Fig. 6, is also evaluated to examine the influence of PSC modelling on hull girder reliability. Due to the lack of detailed documentation on the still water and wave-induced bending moments for this vessel, the mean total bending moment is assumed to be 50 % of the ultimate bending strength (i.e., 50 % × 9.66MNm), calculated based on the nominal design values of the basic geometric and material properties variables. This total bending moment is modelled as a normal distribution with a CoV of 20 % and no uncertainty factor is considered for this total bending moment for simplicity. Based on the specifications by Lua and Hess (2003), the stochastic modelling of geometric parameters, material properties, and the uncertainty factor for ultimate bending strength is consistent with the values listed in Table 2.

4.2. Analysis results

The following four scenarios are considered in FORM-based reliability analysis: 1) considering both χ_e and χ_u, 2) considering χ_u only, 3) considering χ_e only, and 4) considering neither. Fig. 7 illustrates the reliability indices for each scenario across the two case study vessels. The presence of χ_e reduces the reliability index, but its effect is relatively minor when χ_u is included ($\beta = 3.85$ versus $\beta = 3.95$ for the container ship and $\beta = 3.55$ versus $\beta = 3.72$ for the Dow's frigate). However, the effect of χ_e becomes more considerable when χ_u is excluded ($\beta = 5.05$ versus $\beta = 5.33$ for the container ship and $\beta = 4.61$ versus $\beta = 5.32$ for the Dow's frigate). Overall, the inclusion of χ_e represents a reduction of reliability index ranging from 2.5 % to 15 %. This is consistent with observations from the database regarding the specification of the model uncertainty factor χ_e, which shows a negligible bias but notable Coefficient of Variation (CoV).

While the reduction of reliability index is relatively small for the container ship case study, it is notably significant for Dow's frigate, where a 15 % difference in reliability index could substantially influence the decision-making for the design of high-value assets. It is worth noting that the modal uncertainty factor χ_u would only address the uncertainties related to the assumptions of incremental progressive collapse analysis discussed in Section 3.3, if the additional uncertainty

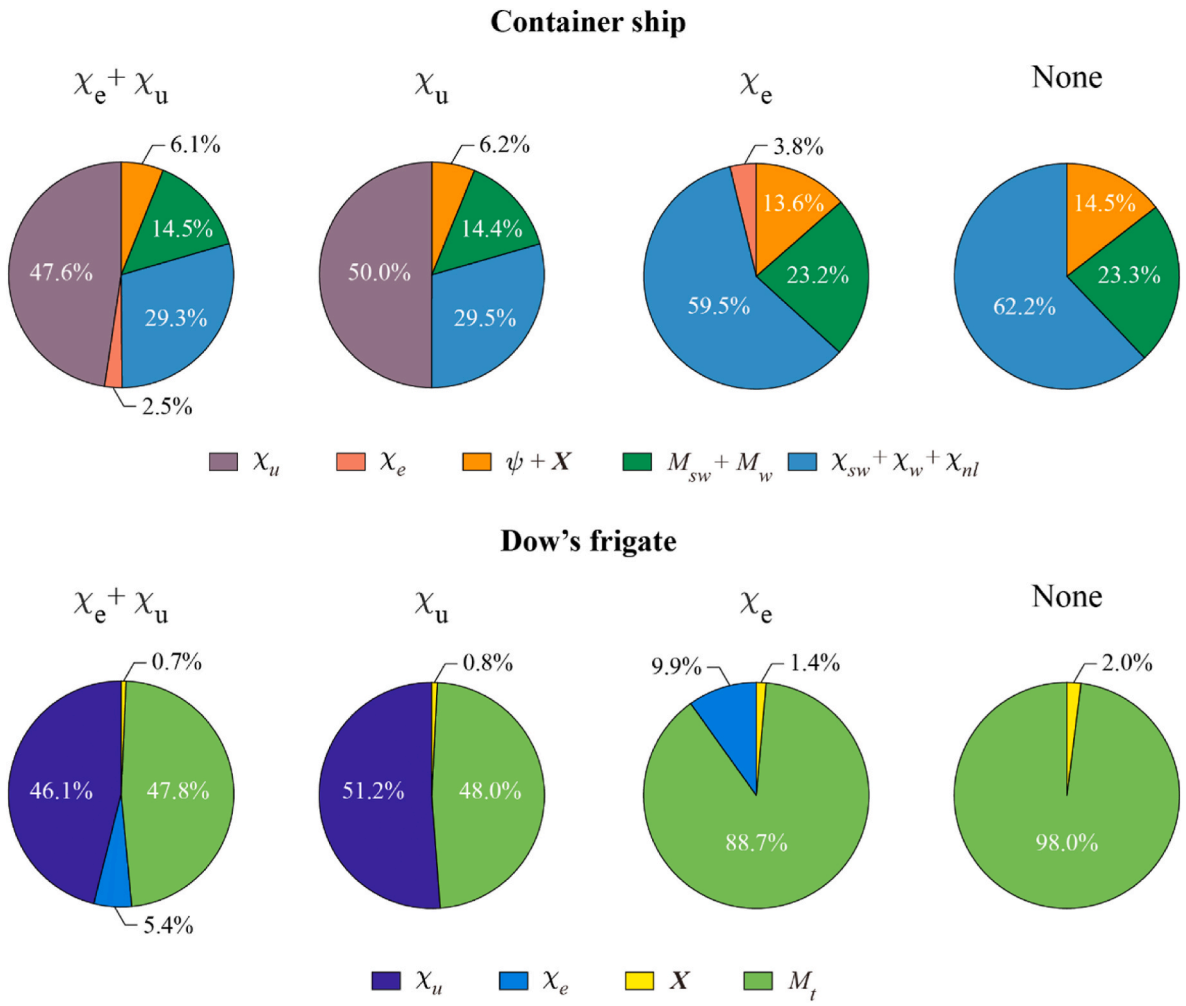

Fig. 8. FORM-based sensitivity factors of container ship and Dow's frigate.

factor χ_e proposed in this study were included. However, in this case study, the uncertainty factor χ_u remains consistent with conventional specifications, meaning the reliability index reduction would be even greater in scenarios where χ_e is also considered. The determination of χ_u in this scenario remains a subject of future research.

To provide further insights into the effects of χ_e, sensitivity factors of random variables obtained from FORM are presented in Fig. 8 for both the container ship and Dow's frigate. These sensitivity factors are expressed as percentages, calculated by squaring the directional cosine. They are herein referred to as the normalised sensitivity factors. The sensitivity factors of certain variables have been grouped together when their individual contributions are small and difficult to visualise. For example, in the container ship analysis, the geometric parameters and material properties are grouped with the load combination factor (denoted as $\psi + \boldsymbol{X}$), the still water and wave-induced bending moments are combined ($\boldsymbol{M}_{sw} + \boldsymbol{M}_w$), and the uncertainty factors of the still water and wave-induced bending moments are merged ($\chi_{sw} + \chi_w + \chi_{nl}$). For the Dow's frigate, only the geometric parameters and material properties (denoted as $\boldsymbol{X}$) are grouped. Consistent with the analysis of the reliability indices, the results indicate that the uncertainty factor χ_u has the dominant influence when included in the analysis, with a normalised sensitivity factor of 47.6 % for the container ship and 46.1 % for Dow's frigate when both χ_u and χ_e are considered. In contrast, the uncertainty factor for PSC elements χ_e, is less influential, with normalised sensitivity

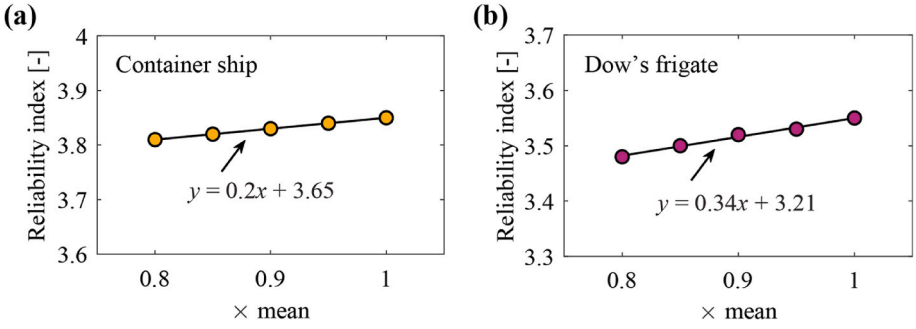

Fig. 9. Effect of the mean value of χ_e on reliability index.

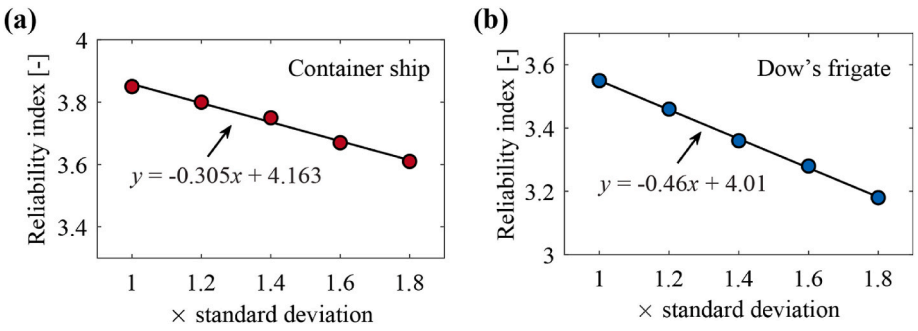

Fig. 10. Effect of the standard deviation of χ_e on reliability index.

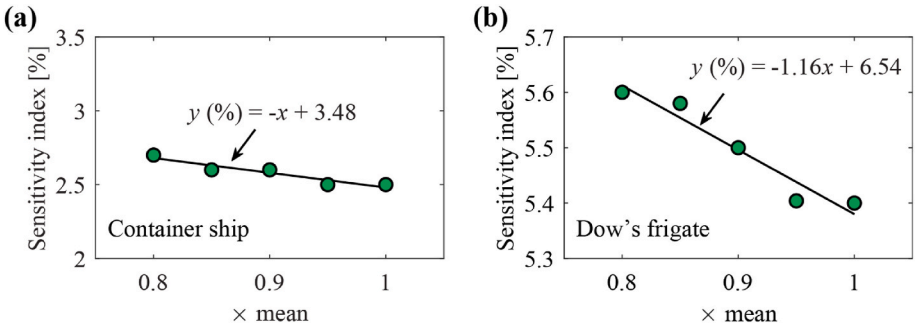

Fig. 11. Effect of the mean value of χ_e on sensitivity factor.

factors of 2.5 % and 5.4 % for the container ship and Dow's frigate, respectively. However, when χ_u is excluded from the analysis, the normalised sensitivity factors of χ_e increase to 3.8 % and 9.9 % for the container ship and Dow's frigate, respectively. Regarding the variables associated with the derivation of PSC load-shortening response (i.e., χ_e and $\boldsymbol{X}$), the results suggest that in these illustrative examples, χ_e has a greater influence than the geometric parameters and material properties. For instance, for Dow's frigate, when χ_u is included in the limit state formulation, the normalised sensitivity factor of χ_e is 5.4 %, compared to only 0.7 % for $\boldsymbol{X}$. When χ_u is excluded, the normalised sensitivity factor of $\boldsymbol{X}$ increases to 1.4 %, compared to 9.9 % for χ_e. Similarly, for the container ship case study, the normalised sensitivity factor of χ_e is 2.5 % when χ_u is included and 3.8 % when χ_u is excluded. In comparison, the normalised sensitivity factor of $\psi + \boldsymbol{X}$ is 6.1 % and 13.6 % for these two cases, respectively. However, most of this contribution comes from the load combination factor (ψ), with the geometric parameters and material properties contributing only 0.2 % and 0.3 %, respectively. Given the negligible magnitude of these values, they are omitted from Fig. 8.

In future work, comparison with experimental data would be beneficial for better quantification of the uncertainty factor. To gain further insight into how variations in the distribution of the model uncertainty factor (which may arise due to the use of different datasets, for example) influence the reliability calculation, parametric analyses are conducted by varying the distribution parameters of χ_e. Specifically, the mean value of χ_e is scaled by factors of 0.8, 0.85, 0.9, and 0.95, while its standard deviation is scaled by factors of 1.2, 1.4, 1.6, and 1.8. Note that only one distribution parameter is varied in each analysis. Figs. 9 and 10 illustrate a nearly linear relationship between the distribution parameters of χ_e and the reliability index. To facilitate comparison, regression lines are fitted to the data, with their slopes indicating the relative influence of each parameter. These best-fit curves are intended solely to support interpretation and are not meant to provide universally applicable design guidance. The results show that variations in the standard deviation have a greater effect on the reliability index than variations in the mean value. Furthermore, the reliability index of Dow's frigate is more sensitive to these variations compared to the container ship. Additionally, Figs. 11 and 12 demonstrate that variations in the distribution parameters can result in sensitivity factors reaching up to 15 %, underscoring their significant role in structural reliability analysis. Regression lines are again fitted to compare the effects of parameter variation. As indicated by their slopes, the sensitivity factor for Dow's frigate exhibits greater variation in response to changes in the distribution parameters compared to the container ship. This greater sensitivity is likely attributed to the slenderer structural configuration of

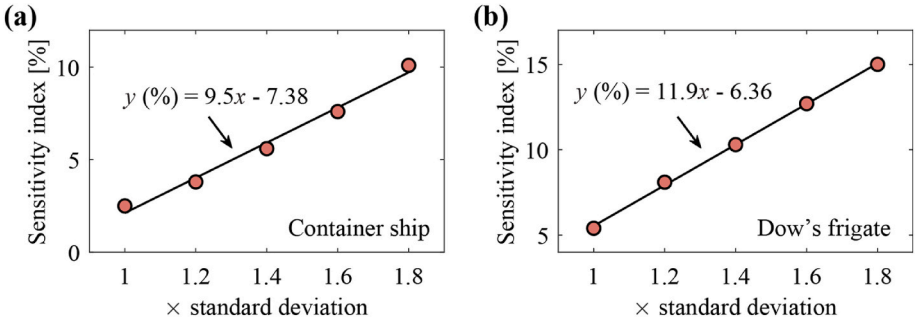

Fig. 12. Effect of the standard deviation of χ_e on sensitivity factor.

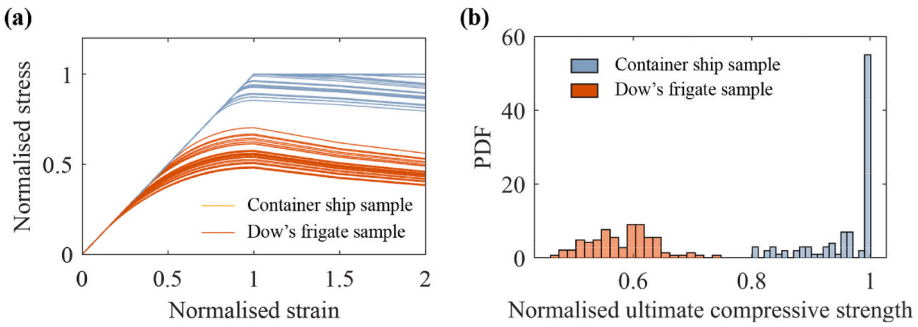

Fig. 13. (a) Illustration of the load-shortening curve samples for primary load-carrying panels in compression; (b) Histogram of the normalised ultimate compressive strength.

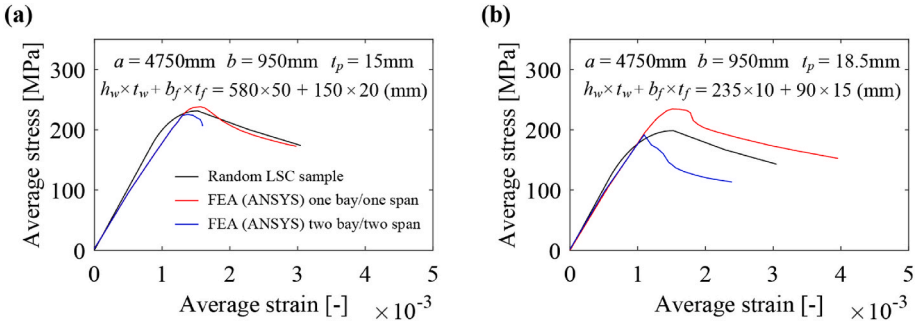

Fig. 14. Comparison with load-shortening curve (LSC) prediction with ISSC benchmark results.

Dow's frigate compared to the container ship. Consequently, its failure is more prone to elastoplastic buckling in compression, making it more sensitive to uncertainties in the prediction of ultimate compressive strength. To illustrate this more clearly, a comparison of load-shortening curve (LSC) sampling is presented in Fig. 13, incorporating the model uncertainty factor χ_e, for the primary load-carrying panels in compression for both vessels. Specifically, the outer bottom panel for the container ship and the deck panel for Dow's frigate. The results show that the ultimate compressive strength of the container ship's primary load-carrying panel is close to the material yield strength (i.e., a normalised ultimate compressive strength near one), resulting in most load-shortening curves nearly resembling elastic-perfectly plastic behaviour, because the ultimate compressive strength should be capped at the material yield strength, regardless of the uncertainty factor χ_e. Conversely, the ultimate compressive strength of Dow's frigate's primary panel is significantly lower than the material yield strength, making it more susceptible to variations in the uncertainty factor χ_e. The histogram of ultimate compressive strength in Fig. 13b further supports this observation. Additionally, the double bottom of the container ship contains a significant number of hard corner elements, which are assumed to exhibit elastic-perfectly plastic behaviour. In contrast, the deck panel of Dow's frigate has only two hard corner elements, located at the intersection of the deck and the side shell. Since these elements are not affected by modelling uncertainties, they remain unchanged regardless of the model uncertainty factor χ_e. Nevertheless, this comparison suggests that different treatments of model uncertainty may be applied for ship hull structures with different characteristics.

4.3. Further discussions

The approach developed in this study establishes a framework to explicitly account for model uncertainty associated with local structural elements, which is a critical input for global hull girder progressive collapse simulations. This paper specifically examines the uncertainty in the maximum load-carrying capacity of PSC elements, or ultimate compressive strength, and its impact on the reliability assessment of ship hull girders. It is important to note again, however, that the stochastic model of χ_e used in this study is illustrative. The findings highlight the potential for a significant impact, but further work is required to quantify this uncertainty factor. Expanding on the collaborative benchmark study by Ringsberg et al. (2021) could provide a pathway to achieving this. Such a study would involve multiple participants providing prediction results based on their best judgment, with comparisons made against baseline data (e.g., controlled experimental results) to derive the uncertainty factor distribution, as exemplified in Fig. 3.

To support the validity of the load-shortening curves modelling, a comparison is provided between a randomly sampled LSC and benchmark results reported in the ISSC (2012) for two PSC elements with different structural configurations. As shown in Fig. 14, the sample LSC exhibits good agreement with finite element predictions obtained using both one bay/one span and two bay/two span models for the case with a relatively strong stiffener (Fig. 14a). For the configuration with a weaker stiffener (Fig. 14b), however, the agreement is less consistent. This reinforces the importance of explicitly accounting for modelling uncertainty in PSC behaviour, particularly since even numerical models (e.g., FEA) can yield divergent results depending on modelling assumptions.

In the derivation of χ_e in the present work, the plate slenderness ratio and column slenderness ratio are used to define the structural configurations. Both parameters are assumed to follow uniform distributions, and 63 cases are generated based on a uniform grid with step sizes of 0.25 (plate slenderness) and 0.1 (column slenderness). An additional analysis has been conducted to confirm that increasing the number of sampled cases does not result in significant changes in the statistical properties of χ_e. This insensitivity is likely attributable to the constrained parameter ranges and the uniform distribution assumption. For future work, there is a clear need to improve the representativeness of the selected cases for uncertainty assessment. This may be achieved through the development of realistic probability distributions for typical plate and column slenderness ratios observed in practice. Such charac-

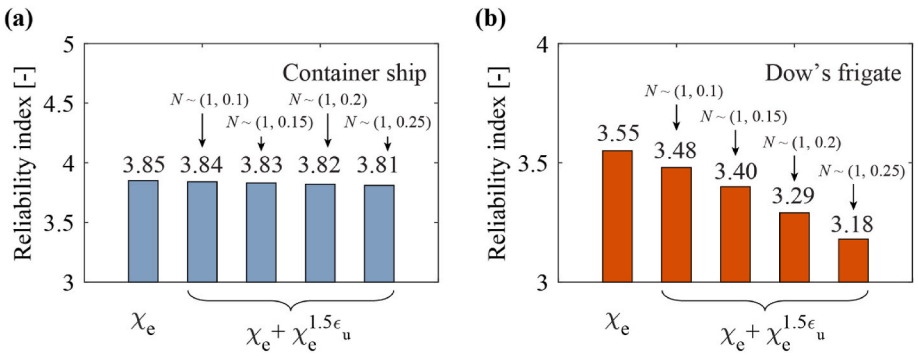

Fig. 15. Effect of the model uncertainty associated with post-collapse response of PSC elements.

terisation would then support the more meaningful application of advanced sampling techniques such as Monte Carlo simulation for deriving model uncertainty factors like χ_e with greater statistical significance (Anyfantis et al., 2023).

Additionally, as noted by Li et al. (2021b), the uncertainty in ultimate compressive strength modelling for PSC elements may substantially vary among structural configurations and slenderness. Stiffened plated structures with higher slenderness tend to exhibit greater uncertainty, whereas stockier structures with lower slenderness ratios typically show comparatively lower uncertainty. Therefore, it might be valuable to establish stochastic models of uncertainty factor for different structural configurations. Furthermore, previous research by Li et al. (2021c) underscores the importance of post-collapse responses in influencing progressive collapse behaviour and ultimate hull girder strength, particularly in naval vessels with lower slenderness (e.g., Dow's frigate). The main reason this effect was not systematically considered in the current paper is that there is still a lack of representative datasets to evaluate this specific uncertainty. Modelling post-collapse responses is anticipated to involve even greater uncertainty, making the PSC element's model uncertainty potentially more significant, and therefore further research in this area is highly valuable. As a preliminary investigation, the model uncertainty associated with the post-collapse response $\sigma_{1.5\varepsilon_u}$ is considered by introducing another model uncertainty factor ($\chi_e^{1.5\varepsilon_u}$). A nominal normal distribution is assumed with a mean value of one and standard deviations of 0.1, 0.15, 0.2, and 0.25. These four different standard deviations aim to illustrate the effect of the post-collapse response. The results, presented in Fig. 15 as a bar chart comparison, demonstrate that the model uncertainty associated with the post-collapse response has a considerable effect on the Dow's frigate. Specifically, the reliability index decreases from an initial value of 3.55 to 3.48 with a modest uncertainty associated with post-collapse response (standard deviation of 0.1) and further reduces to 3.18 under conditions of higher uncertainty (standard deviation of 0.25). Conversely, the effect on container ship is marginal. This disparity is likely caused by the fact that the overall hull girder collapse is dominated by the collapse of critical panels, whereas the Dow's frigate exhibits considerable load-shedding between failed and intact panels. These findings underscore the potentially significant influence of post-collapse response uncertainties on overall reliability assessments, and future systematic research in this area would be valuable.

5. Concluding remarks

This paper presents a methodology to address the uncertainty of PSC modelling into the reliability assessment of ship hull girders under vertical bending. Although the incremental method based on PSC elements has been widely accepted, the model uncertainties associated with the PSC elements and its explicit incorporation in a reliability analysis remain a gap.

Using four empirical formulae and 63 representative combinations of plate and column slenderness ratios, a modelling uncertainty factor χ_e was derived. Illustrative examples of an ultra-large container ship and the Dow's frigate demonstrate this approach. The analysis suggests that the uncertainty factor of PSC modelling χ_e has an appreciable effect on structural reliability, reducing the reliability index by approximately 2.5 %–15 %. The effect is primarily driven by the standard deviation of χ_e rather than its mean value. Additionally, the slenderer structural configuration of the vessel (e.g., the Dow's frigate) is more sceptical to the inclusion of the uncertainty factor χ_e.

Further work is still needed to better quantify this uncertainty factor for all LSC behaviour characteristics. With respect to the uncertainty factor χ_u, it remains necessary to include it in the limit state equation to account for uncertainties associated with the incremental approach, such as cross-section discretisation and other modelling assumptions. However, the level of uncertainty may be reduced with the introduction of the model uncertainty factor χ_e. The extent of this reduction remains an open question for future investigation. A potential approach could involve calibrating χ_u to align the reliability indices obtained with and without incorporating χ_e. This calibration could be performed once an enhanced quantification of χ_e becomes available. Further, this paper examines the impact of PSC modelling on calculating the ultimate hull girder strength reliability under vertical bending, with a particular focus on the uncertainties associated with PSC modelling techniques. Nevertheless, it is evident that modelling uncertainties also stem from other factors such as initial imperfections (e.g., welding-induced deformations and residual stresses), loading types, and age-related deteriorations (e.g., corrosion, fatigue cracking or denting). Further studies are necessary to comprehensively assess these modelling uncertainties.

CRediT authorship contribution statement

Shen Li: Writing – review & editing, Writing – original draft, Visualization, Validation, Software, Resources, Project administration, Methodology, Investigation, Formal analysis, Data curation, Conceptualization. **Jeom Kee Paik:** Writing – review & editing, Writing – original draft, Visualization, Validation, Supervision, Methodology. **C. Guedes Soares:** Writing – review & editing, Writing – original draft, Visualization, Validation, Supervision, Methodology. **Dimitris G. Georgiadis:** Writing – review & editing, Writing – original draft, Visualization, Validation, Methodology, Conceptualization. **Do Kyun Kim:** Writing – review & editing, Writing – original draft, Visualization, Validation, Supervision, Software, Resources, Project administration, Methodology, Investigation, Funding acquisition, Formal analysis, Data curation, Conceptualization.

Declaration of competing interest

No conflict of interest is declared.

Acknowledgement

This research was supported by the Lloyd's Register Foundation (LRF, Grant No. CGY 100002).

Appendix

Table A1
Summary of the dataset for deriving the probability of distribution of uncertainty factor χ_e

No.	β	λ	σ_{xu}^{P-T}	σ_{xu}^{Zhang}	σ_{xu}^{Xu}	σ_{xu}^{Kim}	$\frac{\sigma_{xu}^{Zhang}}{\sigma_{xu}^{P-T}}$	$\frac{\sigma_{xu}^{Xu}}{\sigma_{xu}^{P-T}}$	$\frac{\sigma_{xu}^{Kim}}{\sigma_{xu}^{P-T}}$
1	1.0	0.2	0.9231	0.9971	0.8712	0.8378	1.0802	0.9438	0.9076
2	1.25	0.2	0.8855	0.9367	0.8913	0.8065	1.0579	1.0066	0.9108
3	1.5	0.2	0.8451	0.8901	0.8790	0.7804	1.0532	1.0400	0.9235
4	1.75	0.2	0.8039	0.8525	0.8459	0.7584	1.0604	1.0522	0.9433
5	2.0	0.2	0.7631	0.8212	0.8053	0.7393	1.0761	1.0552	0.9688
6	2.25	0.2	0.7236	0.7946	0.7665	0.7227	1.0981	1.0593	0.9987
7	2.5	0.2	0.6860	0.7715	0.7350	0.7080	1.1246	1.0714	1.0321
8	1.0	0.3	0.9035	0.9896	0.8970	0.8238	1.0953	0.9929	0.9119
9	1.25	0.3	0.8669	0.9296	0.9116	0.7925	1.0724	1.0516	0.9142
10	1.5	0.3	0.8276	0.8834	0.8920	0.7665	1.0673	1.0777	0.9261
11	1.75	0.3	0.7875	0.8460	0.8522	0.7444	1.0743	1.0822	0.9453
12	2.0	0.3	0.7478	0.8150	0.8066	0.7254	1.0899	1.0786	0.9701
13	2.25	0.3	0.7092	0.7885	0.7643	0.7087	1.1118	1.0777	0.9993
14	2.5	0.3	0.6725	0.7656	0.7304	0.6941	1.1384	1.0861	1.0320
15	1.0	0.4	0.8750	0.9744	0.9058	0.8044	1.1136	1.0352	0.9194
16	1.25	0.4	0.8401	0.9154	0.9142	0.7731	1.0896	1.0883	0.9203
17	1.5	0.4	0.8026	0.8698	0.8890	0.7471	1.0837	1.1076	0.9308
18	1.75	0.4	0.7642	0.8331	0.8454	0.7250	1.0901	1.1063	0.9487
19	2.0	0.4	0.7260	0.8025	0.7976	0.7060	1.1053	1.0985	0.9723
20	2.25	0.4	0.6890	0.7765	0.7543	0.6893	1.1269	1.0947	1.0004
21	2.5	0.4	0.6537	0.7539	0.7198	0.6746	1.1533	1.1011	1.0321
22	1.0	0.5	0.8376	0.9497	0.9003	0.7798	1.1338	1.0749	0.9310
23	1.25	0.5	0.8051	0.8921	0.9030	0.7484	1.1081	1.1216	0.9296
24	1.5	0.5	0.7701	0.8477	0.8742	0.7224	1.1009	1.1353	0.9381
25	1.75	0.5	0.7340	0.8119	0.8294	0.7003	1.1061	1.1299	0.9541
26	2.0	0.5	0.6982	0.7821	0.7818	0.6813	1.1203	1.1198	0.9758
27	2.25	0.5	0.6632	0.7568	0.7392	0.6647	1.1410	1.1146	1.0022
28	2.5	0.5	0.6298	0.7348	0.7055	0.6500	1.1667	1.1203	1.0321
29	1.0	0.6	0.7920	0.9148	0.8848	0.7502	1.1550	1.1171	0.9471
30	1.25	0.6	0.7626	0.8594	0.8828	0.7188	1.1269	1.1576	0.9426
31	1.5	0.6	0.7307	0.8166	0.8524	0.6928	1.1176	1.1666	0.9482
32	1.75	0.6	0.6977	0.7821	0.8083	0.6707	1.1210	1.1586	0.9614
33	2.0	0.6	0.6647	0.7534	0.7625	0.6517	1.1335	1.1472	0.9805
34	2.25	0.6	0.6324	0.7290	0.7218	0.6351	1.1527	1.1414	1.0043
35	2.5	0.6	0.6013	0.7078	0.6897	0.6204	1.1770	1.1470	1.0317
36	1.0	0.7	0.7400	0.8706	0.8637	0.7162	1.1765	1.1672	0.9678
37	1.25	0.7	0.7141	0.8179	0.8582	0.6848	1.1454	1.2019	0.9591
38	1.5	0.7	0.6858	0.7772	0.8277	0.6588	1.1333	1.2070	0.9607
39	1.75	0.7	0.6563	0.7443	0.7855	0.6367	1.1341	1.1969	0.9702
40	2.0	0.7	0.6266	0.7170	0.7422	0.6177	1.1442	1.1845	0.9857
41	2.25	0.7	0.5974	0.6938	0.7040	0.6011	1.1613	1.1784	1.0061
42	2.5	0.7	0.5691	0.6736	0.6738	0.5864	1.1835	1.1839	1.0303
43	1.0	0.8	0.6839	0.8193	0.8407	0.6785	1.1980	1.2292	0.9921
44	1.25	0.8	0.6617	0.7697	0.8328	0.6472	1.1633	1.2587	0.9781
45	1.5	0.8	0.6372	0.7314	0.8030	0.6212	1.1478	1.2602	0.9748
46	1.75	0.8	0.6116	0.7005	0.7632	0.5991	1.1454	1.2480	0.9796
47	2.0	0.8	0.5855	0.6748	0.7228	0.5801	1.1526	1.2345	0.9908
48	2.25	0.8	0.5596	0.6529	0.6871	0.5634	1.1668	1.2279	1.0069
49	2.5	0.8	0.5344	0.6339	0.6590	0.5487	1.1863	1.2332	1.0269
50	1.0	0.9	0.6265	0.7639	0.8183	0.6383	1.2193	1.3062	1.0189
51	1.25	0.9	0.6078	0.7176	0.8089	0.6070	1.1806	1.3308	0.9986
52	1.5	0.9	0.5872	0.6819	0.7802	0.5809	1.1614	1.3288	0.9894
53	1.75	0.9	0.5652	0.6531	0.7429	0.5589	1.1554	1.3143	0.9887
54	2.0	0.9	0.5428	0.6291	0.7052	0.5398	1.1591	1.2992	0.9946
55	2.25	0.9	0.5203	0.6087	0.6720	0.5232	1.1699	1.2915	1.0056
56	2.5	0.9	0.4982	0.5910	0.6457	0.5085	1.1863	1.2961	1.0207
57	1.0	1.0	0.5700	0.7071	0.7981	0.5967	1.2406	1.4002	1.0469
58	1.25	1.0	0.5546	0.6643	0.7877	0.5654	1.1977	1.4202	1.0193
59	1.5	1.0	0.5375	0.6312	0.7603	0.5394	1.1744	1.4146	1.0035
60	1.75	1.0	0.5191	0.6046	0.7253	0.5173	1.1646	1.3972	0.9965
61	2.0	1.0	0.5001	0.5824	0.6901	0.4982	1.1646	1.3800	0.9964
62	2.25	1.0	0.4808	0.5635	0.6590	0.4816	1.1719	1.3705	1.0016
63	2.5	1.0	0.4618	0.5471	0.6344	0.4669	1.1848	1.3738	1.0112

References

Adamchak, J.C., 1982. ULSTR: a Program for Estimating the Collapse Moment of a Ship's Hull Under Longitudinal Bending. DTNSRDC report 82/076.

Anyfantis, K.N., Pantazopoulou, S., Papanikolaou, N., 2023. Generalized probabilistic response surfaces for the buckling strength assessment of stiffened panels. Thin-Walled Struct. 189, 110860.

Baarholm, G.S., Moan, T., 2000. Estimation of nonlinear long-term extremes of hull girder loads in ships. Mar. Struct. 13, 495–516.

Bai, Y., Paik, J.K., 2024. Risk Assessment and Management for Ships and Offshore Structures. Elsevier.

Benson, S., Downes, J., Dow, R.S., 2013. Compartment level progressive collapse analysis of lightweight ship structures.". Mar. Struct. 31, 44–62.

Dow, R.S., 1991. Testing and analysis of a 1/3 scale frigate model. In: Advances in Marine Structures, 2. Elsevier, Dunfermline, Scotland, pp. 749–773.

Dow, R.S., 1997. Structural redundancy and damage tolerance in relation to ultimate ship hull strength. In: Advances in marine structures, 3. DERA, Dunfermline, Scotland.

Faisal, M., Noh, S.H., Kawsar, M.R.U., Youssef, S.A.M., Seo, J.K., Ha, Y.C., Paik, J.K., 2017. Rapid hull collapse strength calculations of double hull oil tankers after collisions. Ships Offshore Struct. 12 (5), 624–639.

Faulkner, D., Sadden, J.A., 1979. Toward a Unified Approach to Ship Structural Safety, vol 121. Transaction of Royal Institution of Naval Architects, pp. 1–38.

Francesco, D., Girolami, M., Duncan, A.B., Chryssanthopoulos, M., 2022. A probabilistic model for quantifying uncertainty in the failure assessment diagram. Struct. Saf. 99, 102262.

Fujikubo, M., Alie, M.Z.M., Takemura, K., Iijima, K., Oka, S., 2012. Residual hull girder strength of asymmetrically damaged ships-influence of rotation of neutral axis due to damages. J. Jpn. Soc. Nav. Archit. Ocean Eng. 16, 131–140.

Gaspar, B., Teixeira, A.P., Guedes Soares, C., 2016. Effect of the nonlinear vertical wave-induced bending moments on the ship hull girder reliability. Ocean Eng. 119, 193–207.

Gong, C., Frangopol, D.M., 2020. Time-variant hull girder reliability considering spatial dependence of corrosion growth, geometric and material properties. Reliab. Eng. Syst. Saf. 193, 106612.

Goodman, R.A., 1979. Discussion of Paper "Toward a Unified Approach to Ship Structural Safety, vol 121. Transaction of Royal Institution of Naval Architects, pp. 1–38.

Georgiadis, D.G., Samuelides, E.S., Straub, D., 2023. A Bayesian analysis for the quantification of strength model uncertainty factor of ship structures in ultimate limit state. Mar. Struct. 92, 103495.

Gordo, J.M., Guedes Soares, C., 1996. Approximate method to evaluate the hull girder collapse strength.". Mar. Struct. 9, 449–470.

Guedes Soares, C., Moan, T., 1982. Statistical analysis of still water bending moments and shear forces in tankers, ore and bulk carriers. Norweg. Marit. Res. 3, 33–47.

Guedes Soares, C., 1988. Uncertainty modelling in plate buckling. Struct. Saf. 5 (1), 17–34.

Guedes Soares, C., 1990. Stochastic models of load effects for the primary ship structure. Struct. Saf. 8 (1–4), 353–368.

Guedes Soares, C., Dogliani, M., Ostergaard, C., Parmentier, G., Pedersen, P.T., 1996. Reliability Based Ship Structural Design, vol 104. Transactions of the Society of Naval Architects and Marine Engineers, pp. 357–389.

Guedes Soares, C., Moan, T., 1988. Statistical analysis of still water load effects in ship structures. Trans. - Soc. Nav. Archit. Mar. Eng. 96 (4), 129–156.

Hess, P.E., Bruchman, D., Assakkaf, I.A., Ayyub, B.M., 2002. Uncertainties in material and geometric strength and load variables. Nav. Eng. 114 (2), 139–166.

Hørte, T., Wang, G., White, N., 2007. Calibration of the hull girder ultimate capacity criterion for double hull tankers. In: Proceeding of 10th International Symposium on Practical Design of Ships and Other Floating Structures. Houston, Texas.

Hughes, O.F., 1994. Uncertainty in strength models for marine structures. Ship Struct. Committee.

Hughes, O.F., Paik, J.K., 2010. Ship Structural Analysis and Design. The Society of Naval Architects and Marine Engineers, Alexandria, VA, USA.

IACS, 2019. Common structural rules for bulk carriers and oil tankers. International Association of Classification Societies. London, UK.

Kim, D.K., Lim, H.L., Kim, M.S., Hwang, O.J., Park, K.S., 2017. An empirical formulation for predicting the ultimate strength of stiffened panels subjected to longitudinal compression. Ocean Eng. 140, 270–280.

Kim, D.K., Pedersen, P.T., Paik, J.K., Kim, H.B., Zhang, X.M., Kim, M.S., 2013a. Safety guidelines of ultimate hull girder strength for grounded container ships. Saf. Sci. 59, 46–54.

Kim, D.K., Kim, H.B., Mohd, M.H., Paik, J.K., 2013b. Comparison of residual strength-grounding damage index diagrams for tankers produced by the ALPS/HULL ISFEM and design formula method. Int. J. Nav. Archit. Ocean Eng. 5 (1), 47–61.

Lua, J., Hess, P.E., 2003. Hybrid reliability predictions of single and advanced double-hull ship structures. J. Ship Res. 47 (2), 155–176.

Liu, B., Du, X.K., Gan, J., Ao, L., Wu, W.G., Guedes Soares, C., 2022. Experimental and numerical analysis of the ultimate compressive strength of double-deck structures with a large opening. Ships Offshore Struct. 17 (12), 2788–2801.

Liu, Y., Frangopol, D.M., Cheng, M.H., 2019. Risk-informed structural repair decision making for service life extension of aging naval ships. Mar. Struct. 64, 305–321.

Liu, B., Yao, X.N., Lin, Y.S., Wu, W.G., Guedes Soares, C., 2021. Experimental and numerical analysis of ultimate compressive strength of long-span stiffened panels. Ocean Eng. 237, 109633.

Li, S., Kim, D.K., 2022. A comparison of numerical methods for damage index based residual ultimate limit state assessment of grounded ship hulls. Thin-Walled Struct. 172, 108854.

Li, S., Hu, Z., Benson, S., 2019. An analytical method to predict the buckling and collapse behaviour of plates and stiffened panels under cyclic loading. Eng. Struct. 199, 109627.

Li, S., Hu, Z., Benson, S., 2020. Progressive collapse analysis of ship hull girders subjected to extreme cyclic bending. Mar. Struct. 73, 102803.

Li, S., Kim, D.K., Ringsberg, J.W., Liu, B., Benson, S., 2022. Uncertainty of ship hull girder ultimate strength in global bending predicted by Smith-type collapse analysis. Transactions of the Royal Institution of Naval Architects Part A: Int. J. Maritime Eng. 164 (A2), 185–206.

Li, S., Benson, S., Dow, R.S., 2021a. A Timoshenko beam finite element formulation for thin-walled box girder considering inelastic buckling. Proceeding of 8th International Conference on Marine Structures, Trondheim, Norway.

Li, S., Kim, D.K., Benson, S., 2021b. An adaptable algorithm to predict the load-shortening curves of stiffened panels in compression. Ships Offshore Struct. 16 (Suppl. 1), 122–139.

Li, S., Kim, D.K., Benson, S., 2021c. A probabilistic approach to assess the computational uncertainty of ultimate strength of hull girders. Reliab. Eng. Syst. Saf. 213, 107688.

Mansour, A.E., 1972. Probabilistic Design Concepts in Ship Structural Safety and Reliability, vol. 80. Transaction of Society of Naval Architects and Marine Engineers, pp. 64–97.

Magoga, T., Flockhart, C., 2014. Effect of weld-induced imperfections on the ultimate strength of an aluminium patrol boat determined by the ISFEM rapid assessment method. Ships Offshore Struct. 9 (2), 218–235.

Mohammed, E.A., Benson, S.D., Hirdaris, S.E., Dow, R.S., 2016. Design safety margin of a 10,000 TEU container ship through ultimate hull girder load combination analysis. Mar. Struct. 46, 78–101.

Moan, T., 1979. Discussion of Paper "Toward a Unified Approach to Ship Structural Safety, vol 121. Transaction of Royal Institution of Naval Architects, pp. 1–38.

Paik, J.K., 2018. Ultimate Limit State Analysis and Design of Plated Structures, second ed. John Wiley & Sons, Chichester, UK.

Paik, J.K., 2020. Advanced Structural Safety Studies with Extreme Conditions. Springer, Singapore.

Paik, J.K., 2022. Ship-Shaped Offshore Installations: Design, Construction, Operation, Healthcare and Decommissioning, second ed. Cambridge University Press, Cambridge, UK.

Paik, J.K., Thayamballi, A.K., 1997. An empirical formulation for predicting the ultimate compressive strength of stiffened panels. Proceedings of 7th International Offshore and Polar Engineering Conference (ISOPE), Honolulu, Hawaii.

Paik, J.K., Frieze, P.A., 2001. Ship structural safety and reliability. Prog. Struct. Eng. Mater. 3 (2), 107–210.

Paik, J.K., Kim, D.K., Park, D.H., Kim, H.B., Mansour, A.E., Caldwell, J.B., 2012. Modified paik-mansour formula for ultimate strength calculations of ship hulls. Ships Offshore Struct. 8 (3–4), 245–260.

Paik, J.K., Lee, D.H., Noh, S.H., Park, D.K., Ringsberg, J.W., 2020. Full-scale collapse testing of a steel stiffened plate structure under axial-compressive loading triggered by brittle fracture at cryogenic condition. Ships Offshore Struct. 15 (Suppl. 1), 29–45.

Parunov, J., Guedes Soares, C., 2008. Effects of common structural rules on hull-girder reliability of an aframax oil tanker. Reliab. Eng. Syst. Saf. 93 (9), 1317–1327.

Parunov, J., Guedes Soares, C., Hirdaris, S., Wang, X.L., 2022. Uncertainties in modelling the low-frequency wave-induced global loads in ships. Mar. Struct. 86, 103307.

Parunov, J., Prebeg, P., Rudan, S., 2020. Post-accidental structural reliability of double-hull oil tanker with near realistic collision damage shapes. Ships and Offshore Struct. 15 (supp 1), 190–207.

Rackwitz, R., Fiessler, B., 1978. Structural reliability under combined random load sequences. Comput. Struct. 1978 (5), 484494.

Ringsberg, J.W., Darie, I., Nahshon, K., Shilling, G., Vaz, M.A., Benson, S., Brubak, L., Feng, G.Q., Fujikubo, M., Gaiotti, M., Hu, Z.Q., Jang, B.S., Paik, J.P., Slagstad, M., Tabri, K., Wang, Y.K., Wiegard, B., Yanagihara, D., 2021. The ISSC 2022 committee III. 1-Ultimate strength benchmark study on the ultimate limit state analysis of a stiffened plate structure subjected to uniaxial compressive loads. Mar. Struct. 79, 103026.

Shu, Z., Moan, T., 2011. Reliability analysis of a bulk carrier in ultimate limit state under combined global and local loads in the hogging and alternate hold loading condition. Mar. Struct. 24 (1), 1–22.

Smith, C.S., 1977. Influence of local compressive failure on ultimate longitudinal strength of a ship's hull. Proceeding of 1st International Symposium on Practical Design of Ships and Other Floating Structures, Tokyo, Japan.

Smith, C.S., Dow, R.S., 1986. Ultimate Strength of a Ship's Hull Under Biaxial Bending. Admiralty Research Establishment. ARE TR 86204.

Tatsumi, A., Htoo, H., Ko, H., Fujikubo, M., 2020. Ultimate strength of container ships subjected to combined hogging moment and bottom local loads, part 2: an extension of smith' s method. Mar. Struct. 71, 102738.

Teixeira, A.P., Guedes Soares, C., Chen, N.Z., Wang, G., 2013. Uncertainty analysis of load combination factors for global longitudinal bending moments of double hull tankers. J. Ship Res. 57 (1), 42–58.

Wang, X., Moan, T., 1996. Stochastic and deterministic combinations of still water and wave bending moments in ships. Mar. Struct. 9, 787–810.
Xu, M.C., Song, Z.J., Zhang, B.W., Pan, J., 2018. Empirical formula for predicting ultimate strength of stiffened panel of ship structure under combined longitudinal compression and lateral loads. Ocean Eng. 162, 161–175.
Xu, M.C., Teixeira, A.P., Guedes Soares, C., 2015. Reliability Assessment of a Tanker Using the Model Correction Factor Method Based on the IACS-CSR Requirement for Hull Girder Ultimate Strength.
Youssef, S.A.M., Faisal, M., Seo, J.K., Kim, B.J., Ha, Y.C., Kim, D.K., Paik, J.K., Cheng, F., Kim, M.S., 2016. Assessing the risk of ship hull collapse due to collision. Ships Offshore Struct. 11 (4), 335–350.
Youssef, S.A.M., Noh, S.H., Paik, J.K., 2017. A new method for assessing the safety of ships damaged by collision. Ships Offshore Struct. 12 (6), 862–872.
Zhang, X.M., Paik, J.K., Jones, N., 2016. A new method for assessing the shakedown limit state associated with the breakage of a ship's hull girder. Ships Offshore Struct. 11 (1), 92–104.
Zhang, S., Khan, I., 2009. Buckling and ultimate capability of plates and stiffened panels in axial compression. Mar. Struct. 22, 791–808.